DESIGN OF COMPLIANT MECHANISMS BASED ON RIGID-BODY MECHANISMS

LENA ZENTNER[1]; STEFAN HENNING[1]; THOMAS FRÖHLICH[2]

Abstract. The design of compliant mechanisms is a much more complicated task than their analysis. Consequently, there are many more methods available for the analysis of compliant mechanisms than for their synthesis. In this article, a contribution to the synthesis of compliant mechanisms is made by presenting a comparison of two different methods for their design. In both methods rigid-body systems are used as a basis for compliant mechanisms. Depending on the task of the compliant mechanism, one of these methods can be selected and applied. The deviations between the results of the used theory and measurement results as well as FEM results are less than 5.5 % for displacements and acting forces. Selected mechanisms for the realization of a straight-line motion of a point and for given relative motions are presented as examples.

Key words: Compliant mechanisms, compliant joints, design of compliant mechanisms, calculating tools.

1. INTRODUCTION

Compliant mechanisms are increasingly utilized in precision engineering, micro mechanics and other fields of applications due to their advantages like high reproducibility, high resolution or clearance-free and friction-less motion. Despite a large number of approaches for the analysis of their deformation behavior, synthesis methods are rather limited and sometimes specific to a certain configuration. In literature a variety of different approaches for the compliant mechanism design exist. Overviews are given in [1] and [2]. Some well-established synthesis methods include specific design equations (e.g. [3]) providing closed-form solutions for flexure hinges or mechanisms. Also, the rigid-body-replacement method (e.g. [4]) for replacing conventional hinges by flexure hinges with concentrated or distributed compliance is often used. Further methods include the building-block approaches where basic mechanism blocks are connected in a certain way to fulfill a desired displacement (e.g. [5]) or building blocks arranged in a meshed design domain where an optimal topology is found for defined inputs and outputs (e.g. [6]).

[1] Compliant Systems Group, Technische Universität Ilmenau, Germany
[2] Process Measurement Group, Technische Universität Ilmenau, Germany

Ro. J. Techn. Sci. − Appl. Mechanics, Vol. 67, N° 1, P. 61−78, Bucharest, 2022

Moreover, approaches based on structural optimization usually based on finite elements (FE) methods (e.g. [7]) are commonly used. Rarely, analytical models are used for synthesis to design a variety of different compliant mechanisms. In this paper, two synthesis methods are presented based on rigid-body-replacement. For the first method, non-linear beam theory is applied for the numerical calculation of arbitrary compliant mechanisms with concentrated compliance. For the second method linear beam theory is utilized providing analytical solutions for compliant mechanisms with concentrated and distributed compliance. The use of graphical user interfaces enables an easy utilization of the mentioned analytical methods.

2. METHOD 1: SYNTHESIS METHOD FOR A PREDETERMINED BEHAVIOR OF COMPLIANT MECHANISMS

The first method is based on the non-linear theory for large deflections of rod-like structures [8]. In a first step, Fig. 1, (1) a suitable rigid-body mechanism with desired properties is found. Then (2) its rotational joints are replaced by flexure hinges. Next (3), their individual contour design and geometric parameters are synthesized using the theory for large deflections. After that, (4) the flexure hinges are integrated into the new compliant mechanism [9]. Finally, the resulting compliant mechanism can be optimized by also using the theory for large deflections to improve the desired properties [10]. With this method, only kinematic properties of the mechanisms are considered.

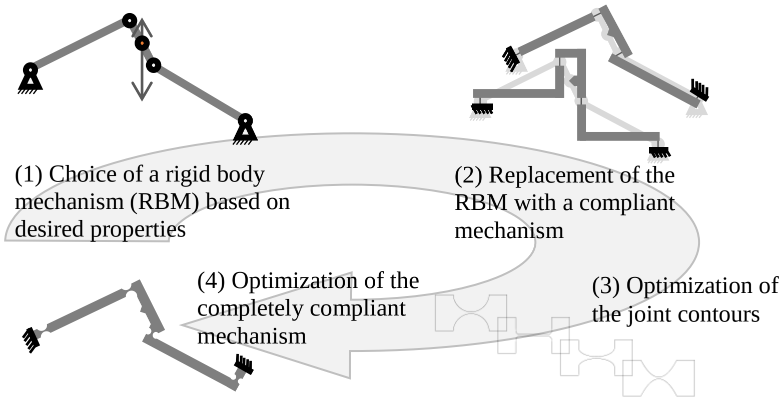

Fig. 1 – Synthesis method for creating the compliant mechanisms for a given behavior, e.g., for a given trajectory of a point.

In the first step, it is assumed that a set of rigid body mechanisms in the form of a catalog is available to choose a suitable mechanism. It is advantageous if the mechanisms can be arranged in such a catalog according to desired properties.

Such a collection of mechanisms can be found at https://www.dmg-lib.org at the Digital Mechanism and Gear Library (DMG-Lib). Mechanisms can be searched here according to various parameters and properties, such as name of mechanism, direction of the path, orientation of output link, trace of a dedicated point on follower, form of transfer function etc. An example of a plane mechanism is considered, where the straight-line guidance of a point is to be realized. In DMG-Lib, a slider-crank mechanism can be found, Fig. 2, if the name of the mechanism (slider-crank mechanism) and the trace of a dedicated point on the follower (straight-line motion) are entered in the search criteria. The dimensions and location of the mechanism are then determined. The decision for this depends mainly on the assembly space and the range of motion. For the length of the path of point P, 5 mm is chosen. The following coordinates are set:

Joint 1:	(0 mm, 0 mm)
Joint 2:	(30 mm, 50 mm)
Joint 3:	(60 mm, 0 mm)
Point P:	(0 mm, 100 mm)

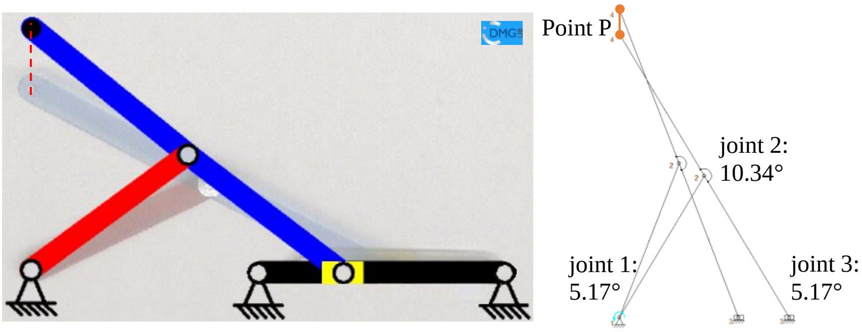

Fig. 2 – Rigid-body mechanism with a straight-line guidance (DMG-Lib) of a point and its model in SAM.

Next, relative angles in each pivot joint are determined. This can be calculated or found very quickly using software suitable for this purpose, such as SAM (Simulation and Analysis of Mechanisms), Fig. 2. For a straight path of 5 mm of a point P, relative angles of 5.17°, 10.34° and 5.17° (rounding to two decimal digits) are realized in the joints 1, 2 and 3, respectively.

Now, in the second step, these pivot joints are to be replaced by the compliant joints, Fig. 3. This is an intuitive process, but the following rules can be recommended:

- it is preferable to introduce compliant joints with concentrated compliance (because of smaller displacements of the axis of rotation);
- the center of the beam axis of the compliant joint should be coincident with the axis of rotation of the pivot joint;

- the compliant joints must be oriented in the compliant mechanism so that they are loaded mainly by bending;
- at least half a length of the joint contour must be provided on both its sides;
- for the beam axes of the compliant mechanism links, the shortest distances are to be chosen.

A possible compliant mechanism is shown in Fig. 3.

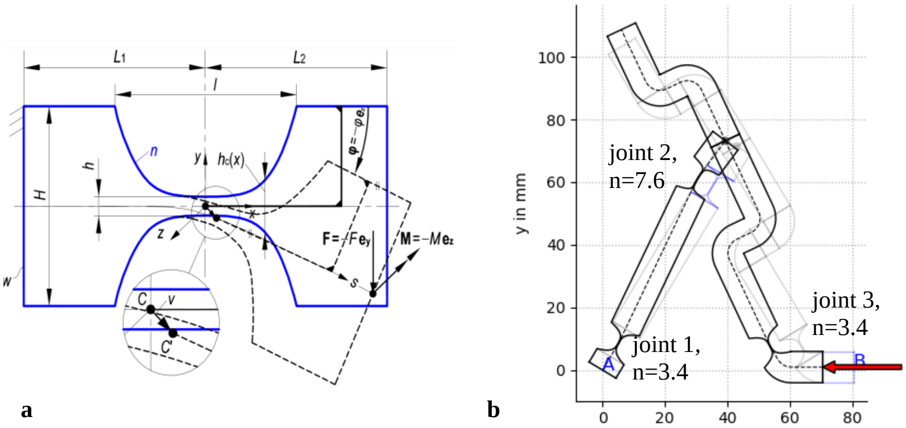

Fig. 3 – A compliant joint (a) and a possible mechanism based on the rigid-body mechanism of Fig 2 (b).

In the third step, compliant joints are dimensioned. For this purpose, the theory for large deflections of curved beams is applied. The bending angle θ, as an angle between the tangent to the beam axis and the *x*-axis, can be related to the external force F_L by the following equations:

$$\frac{dM}{ds} = F_L \sin(\theta - \alpha),$$
$$\frac{d\theta}{ds} = \frac{M}{EI_Z(s)} + \kappa_0(s), \tag{1}$$

with the boundary conditions:

$$M(L) = M_L, \quad \theta(0) = 0. \tag{2}$$

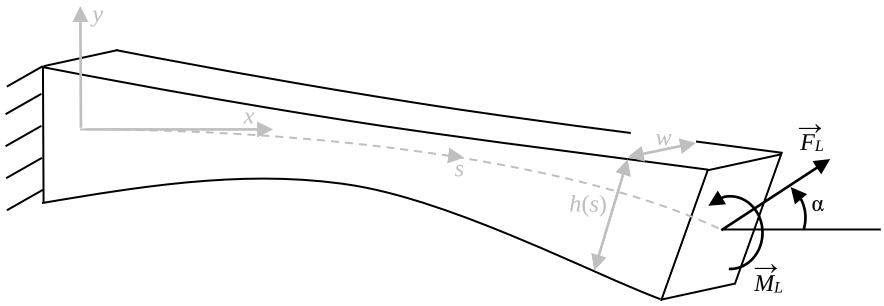

Fig. 4 – A compliant joint with model parameters.

If the joints are prismatic, then the parameters w and $h(s)$ describe the cross-sectional area of the joint and are included in the parameter I_Z, as the second moment of area. The coordinate s is measured along the beam axis. At the end of the clamped joint a moment M_L and a force F_L are applied. The force forms an angle α with the x-axis. E is the YOUNG's modulus of the material. The beam axis of the compliant joint may have an initial curvature κ_0. An additional condition (3) should be used when determining an unknown geometrical parameter.

$$\theta(L) = \theta_L . \tag{3}$$

There are at least two special cases that allow to write down an analytical solution. In the first special case, only one moment M_L ($F_L = 0$) acts on the joint. Then the following solution can be found for the angle θ:

$$\theta(s) = \frac{M_L}{E} \int \frac{ds}{I_Z(s)} + \int \kappa_0(s) ds + C_1 \tag{4}$$

or for the prismatic joints:

$$\theta(s) = \frac{12 M_L}{wE} \int \frac{ds}{h^3(s)} + \int \kappa_0(s) ds + C_1 . \tag{5}$$

If the integrals in (5) can be found, then the integration constant from the second condition in (2) can also be determined. In addition, the condition for the strain ε is considered:

$$|\varepsilon|_{\max} = \frac{6|M_L|}{Ewh_{\min}{}^2} \le \varepsilon_{zul.} \tag{6}$$

S is a safety factor in this case. To determine a geometrical parameter of the joint contour, the following condition (7) can be used. It is based on equation (5), inequation (6) and on condition (3).

$$\theta_L \le \frac{2\varepsilon_{zul.}h_{\min}^2}{S}\int \frac{ds}{h^3(s)}\bigg|_{s=L} + \int \kappa_0(s)ds\bigg|_{s=L} + C_1, \quad M_L > 0\,. \tag{7}$$

Another case, which allows an analytical solution, is when κ_0 and I_Z are constant. Then the equations (1) can be reduced to the following equation:

$$\frac{d^2\theta}{ds^2} = \frac{F_L \sin(\alpha-\theta)}{EI_Z}\,. \tag{8}$$

The solution of this equation can be written down for s by an elliptic integral of the first kind, denoted here by F_{El}:

$$s = \mp\frac{2F_{El}(\frac{\alpha-\theta}{2},\frac{2k}{c+k})}{\sqrt{c+k}}, \quad "-"\ \text{for}\ \frac{d\theta}{ds} \ge 0, \quad "+"\ \text{for}\ \frac{d\theta}{ds} < 0\,, \tag{9}$$

with the constants:

$$k = \frac{2F_L}{EI_Z}, \quad c = \left(\frac{M_L}{EI_Z} + \kappa_0\right)^2 - k\cos(\alpha-\theta_L)\,. \tag{10}$$

In this case, for example, the length of the joint can be found for the bending angle if other parameters are known:

$$L = \mp\frac{2F_{El}(\frac{\alpha-\theta_L}{2},\frac{2k}{c+k})}{\sqrt{c+k}}\,. \tag{11}$$

However, the parameters of the contour cannot be determined analytically here. The determination of the joint contour, especially by analytical means, is only possible for special cases. In order to consider general cases and to minimize the time for the determination of the joint contour, the tool "detasFLEX" was developed. Four different joint contours are implemented in this tool: circular, corner-filleted, elliptical and power function, Table 1.

The tool is based on the theory for large deflections of curved beams, solving equations (1) and (2) numerically. For this purpose, MATLAB was used as a stand-alone software application, requiring only the license-free runtime environment. Geometric and material parameters of the joint are used as input parameters. The calculation is possible for a bending moment and a shear force as well as a combination of the two loads. The calculation of the results can be output either for three load cases or for a given bending angle up to 45°. A wide range of result parameters can be calculated and the most important joint properties, such as the deformed beam axis, the bending stress, the rotational accuracy and the elastic strain distribution are displayed in the form of diagrams. In addition, a preview of the exact joint geometry with the instant visualization is implemented in the tool. In addition, values for the angle or for the load, the axis displacement, the strain distribution, the maximum strain and the maximum possible bending angle are calculated. Validation of the modeling based on the theory for large deflections of curved beams is described in section 4.

Table 1

Four different joint contours and their mathematical description.

Joint contour	image	formula
circular	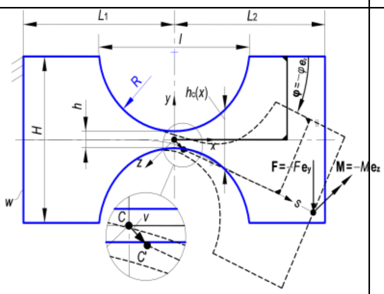	$h_0 + 2R - 2\sqrt{R^2 - x^2}$, with $R = 0.5l$
corner-filleted	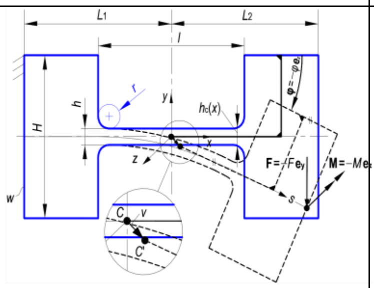	$h_0 + 2r - 2\sqrt{r^2 - (x + l/2 - r)^2}$, $-l/2 \le x < -l/2 + r$, h_0 , $-l/2 + r \le x \le l/2 - r$ $h_0 + 2r - 2\sqrt{r^2 - (x - l/2 + r)^2}$, $l/2 - r < x \le l/2$ with $r = 0.1l$
elliptical	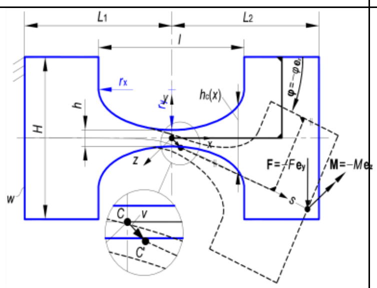	$h_0 + 2r_y\left(1 - \sqrt{1 - \frac{x^2}{{r_x}^2}}\right)$, with $r_x = 0.5l$ and $r_y = 0.25l$

power function	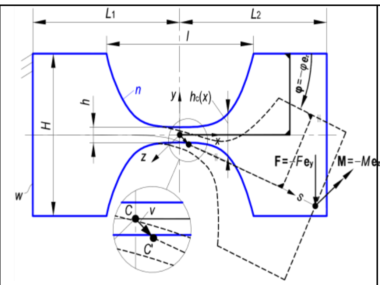	$h_0 + \frac{(H-h_0)}{(l/2)^n}\lvert x\rvert^n,$ $n \geq 2$

DetasFLEX provides a variety of different geometry, material and contour configurations as well as multiple analysis criteria and settings. This allows numerous compliant joints for different tasks to be analyzed accurately within a few seconds. In this way, each joint in a compliant mechanism can be designed in a targeted and individual manner. Based on this, PC-based synthesis is also possible in conjunction with the analysis part of the tool. DetasFLEX-analysis is freely available at "https://www.tu-ilmenau.de/nsys/tools/detasflex-analysis".

In the example considered, relative angles of 5.17°, 10.34° and 5.17° are to be realized by the compliant joints. The goal is to achieve a minimal rotational axis shift and for this example at a safety factor of at least S = 1.2 related to the maximum allowable strain $\varepsilon_{all.}$. The supposition of a safety factor allows an additional margin in the final optimization of the whole mechanism. The application of the DetasFLEX tool with the choice of the polynomial function gives results shown in Table 2.

Table 2

The results of using the DetasFLEX tool with the choice of the polynomial function.

Joint	Power *n*	Force in N	Rotat. axis shift in mm
1, 3	3.4	1.18	0.006
2	7.6	1.05	0.044

The following parameters were used:

$$\begin{aligned} &H = 10\text{ mm}, \quad h_0 = 0.2\text{ mm}, \quad L_1 = L_2 = 10\text{ mm}, \\ &l = 10\text{ mm}, \quad w = 6\text{ mm}, \quad E = 72000\text{ MPa}, \quad \varepsilon_{all.} = 0.5\,\%. \end{aligned} \tag{12}$$

The smaller the polynomial power n of $h(s)$, the smaller the shift of the rotation axis but the larger the maximum strain in the joint.

The last step is to check the behavior of the compliant mechanism. For this purpose, the tool CoMUI (Design tool for the analysis and synthesis of compliant mechanisms) can be used. This tool is also freely available at "https://www.tu-ilmenau.de/nsys/tools/comui". The tool is also based on the theory for large deflections of curved beams like detasFLEX and is organized analogously. The tool was developed in Python and represents a standalone application.

The compliant mechanism consists of three parts, which in turn are divided into individual sections. The sections are straight or curved with constant curvatures. The dimensions of the lengths of individual sections can be found in Table 3. The deformation of the mechanism is calculated with the help of the tool under the action of a force of 0.45 N. This is approximately one third of the force acting on each of the three joints, but with the angle between the force and the joint axes taken into account. The point P of the mechanism is displaced by about 5.3 mm in y-direction and has a deviation from the straight path (displacement in x-direction) of about 0.158 mm. The maximum strain of approx. 0.455 % is reached at joint 3.

Table 3

The length dimensions of individual sections of the compliant mechanism.

<table>
<tr><th rowspan="2">Part</th><th rowspan="2">Image</th><th colspan="8">Length of the element in mm</th></tr>
<tr><th>1</th><th>2</th><th>3</th><th>4</th><th>5</th><th>6</th><th>7</th><th>8</th></tr>
<tr><td rowspan="2">1</td><td rowspan="2">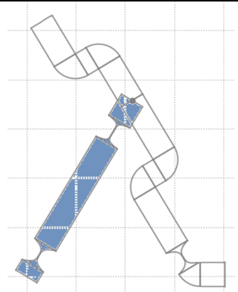</td><td>5</td><td>10</td><td>48.3</td><td>10</td><td>10</td><td>-</td><td>-</td><td>-</td></tr>
<tr><td colspan="8">counted from the clamping</td></tr>
<tr><td rowspan="2">2</td><td rowspan="2">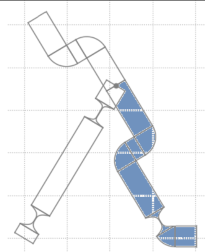</td><td>25</td><td>7.85</td><td>5</td><td>7.85</td><td>25.4</td><td>10</td><td>5.15</td><td>10</td></tr>
<tr><td colspan="8">counted from branching point</td></tr>
<tr><td rowspan="2">3</td><td rowspan="2">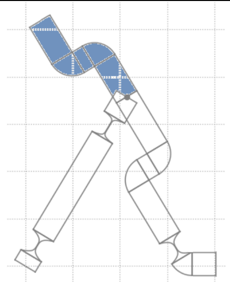</td><td>18</td><td>7.85</td><td>5</td><td>7.85</td><td>18.3</td><td>-</td><td>-</td><td>-</td></tr>
<tr><td colspan="8">counted from branching point</td></tr>
</table>

In the "Parametric Study" part of the tool, selected parameters can be varied in a given range. For the obtained mechanism, there is a possibility, for example, to change the polynomial power *n* of the contour of the joint 2 to reduce the deviation from the straight path. The new result for the power is n = 10.6. The deviation is reduced to 0.147 mm, with the path length then reaching 5.75 mm and the maximum strain approx. 0.5 % also reaching the maximum allowable strain in joint 3. Other geometric parameters or elastic modulus and the applied force can also be varied to minimize the deviation from the straight path. Further optimization steps will not contribute significantly to the demonstration of this synthesis method, so they are omitted here.

3. METHOD 2: SYNTHESIS METHOD FOR A GIVEN RELATIVE MOTION OF THE COMPLIANT MECHANISM PARTS

The second method is based on the linear theory of straight beams. In the method, the approach for modeling a compliant mechanism as a rigid-body model is used [8]. Here, the compliant sections, as beam elements, Fig. 5, are identified and replaced by rigid-body elements, which are connected by a pivot joint and a torsion spring. Three different types of load at the end of a compliant beam element are considered: Loading by moment (k = 1), by force (k = 2) and by distributed force (k = 3). The modeling consists in finding the position of the joint, described by δ, and the value of the spring constant c_t in such a way (13) that the displacement in *y*-direction and the bending angle are the same for both systems, compliant element and its rigid model, Fig. 5.

$$\delta = \frac{\sum_{k=1}^{3} \frac{M_k{}^H}{k+1}}{\sum_{k=1}^{3} \frac{M_k{}^H}{k}}, \quad c_t = \frac{EI_z}{L} \cdot \frac{\sum_{k=1}^{3} M_k{}^H \cdot \delta^{k-1}}{\sum_{n=1}^{3} \frac{M_k{}^H}{k}}, \tag{13}$$

$$\text{with} \quad M_1{}^H = M_L, \quad M_2{}^H = lF_L, \quad M_3{}^H = \frac{q_L l^2}{2}.$$

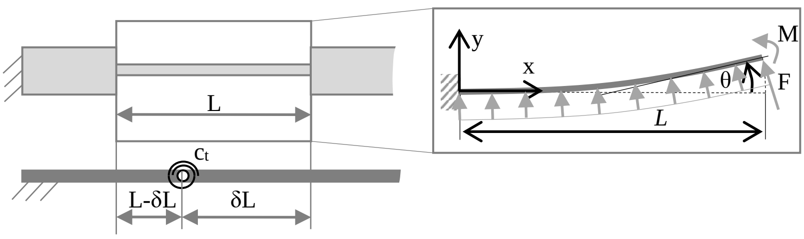

Fig. 5 – To build the model: Replace compliant sections with rigid-body elements connected by a swivel joint and a torsion spring.

This approach, but in reverse, can be used to synthesize compliant mechanisms. As in the first synthesis method, a suitable rigid-body mechanism is first selected. Then, desired hinges are replaced with compliant elements. In the next step, the compliant mechanism is dimensioned according to (13). Finally, the obtained compliant mechanism can be tested or optimized if necessary, Fig. 6. In contrast to the first method, the value and type of load play a significant role here, since the position of the joint and thus the relative movement of the system parts to each other are determined depending on this.

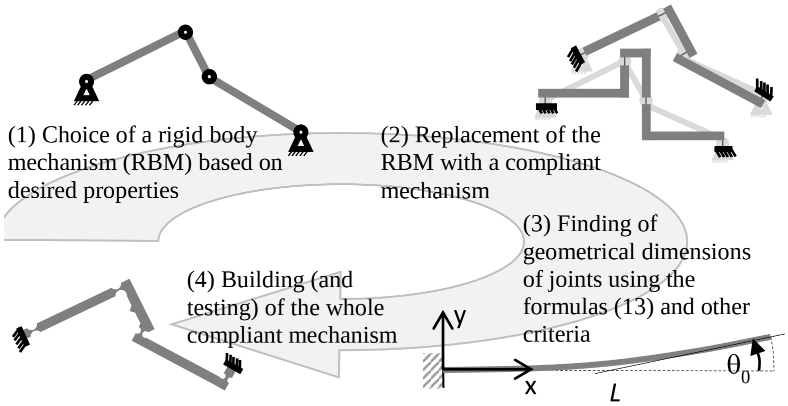

Fig. 6 – Synthesis method for designing mechanisms for a given relative motion of mechanism parts to each other.

This method is very suitable when, for example, a rigid-body mechanism is to be replaced by a more compliant mechanism. Here, a mechanism from a car seat is considered as an example. A four-link mechanism is installed in a car seat. It transmits an actuating force F from the person to adjust the back of the seat. A spring returns it to its original position after actuation. To reduce the number of components (pivot elements, return spring), a partially compliant mechanism with at least one compliant joint is to be developed Fig. 7.

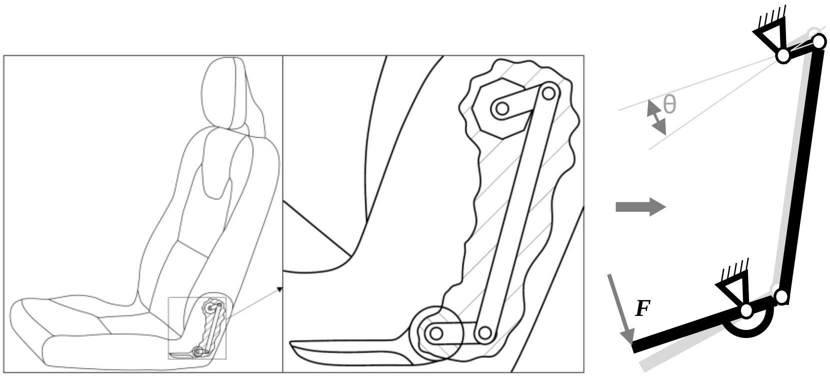

Fig. 7 – An example of a rigid-body mechanism from a car seat.

In this case, when the mechanism is already given, the first step of the synthesis, Fig. 6, is skipped. Loads corresponding to the mentioned types n =1,2,3 are determined. Since axial forces are not considered in this theory, they are not determined. Also for this reason, it is recommended to choose the orientation of compliant joints in such a way that the axial forces exert only minor effects or no effect at all. In the given mechanism, only one joint should be replaced by a compliant connection, while other parts of the mechanism should continue to be used. The orientation of the compliant joint coincides with the orientation of the corresponding rigid-body link, Fig. 8. The compliant joint is modeled as a clamped beam on which a force F_L and a moment M_L act:

$$F_L = F\frac{c}{a}, \quad M_L = F_L(a - \delta L)\,. \tag{14}$$

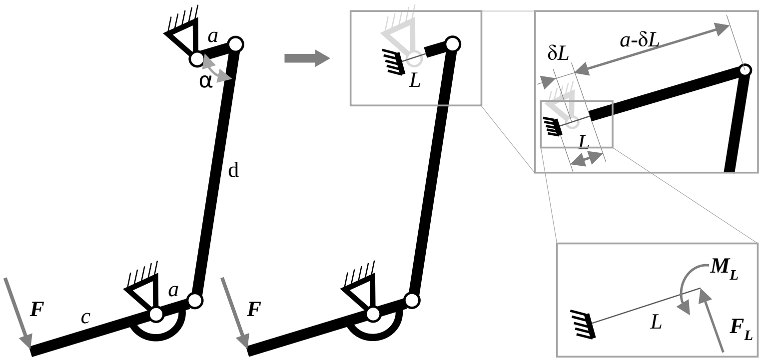

Fig. 8 – Presentation for replacing a pivot joint of a rigid body mechanism with a compliant joint.

Under the force of F = 5 N, the output link should realize an angle of θ = 20°, Fig. 7. For a rigid-body model as in Fig. 5, the following applies to the bending angle:

$$\theta = \frac{F_L(a-\delta L)+F_L L\delta}{c_t}. \tag{15}$$

In addition, the strain should be limited:

$$\varepsilon_{\max} = 6\frac{M_L + F_L L}{Ewh^2} \le \varepsilon_{all.} \tag{16}$$

For a desired maximum strain $\varepsilon_0 \le \varepsilon_{\text{all.}}$ the following then applies:

$$\varepsilon_0 = 6\frac{M_L + F_L L}{Ewh^2}. \tag{17}$$

The parameters h and w are the dimensions of the cross-sectional area. The following geometrical and material parameters are assumed:

$$\begin{aligned} &a = 20\text{ mm}, \quad c = 80\text{ mm}, \quad h = 0.5\text{ mm},\\ &\varepsilon_0 = 0.01, \quad E = 210000\text{ N/mm}^2. \end{aligned} \tag{18}$$

Consequently, the length L, width w and the position of the joint, described by δ, are looked for. The relations (15), (17) as well as the formulas (13) considering (14) and (18) allow to determine these parameters. The equations can be solved analytically. Therefore, a different choice of the parameters can be searched. For the considered problem there are several solutions, one of the solutions is given in (19).

$$L \approx 6\text{ mm}, \quad \delta \approx 0.53, \quad w \approx 3\text{ mm}. \tag{19}$$

A test using linear theory assuming the parameters from (18) and (19) (not rounded) with the force of 5 N gives exactly 20°, since linear theory was used as the basis for this synthesis method. As long as the linear theory can be accepted for the given deformations, this method gives good results. The application of the non-linear theory according to (1) with α = 90° results in approx. 18°.

In another example, a four-link mechanism serves as a model for a compliant beam-shaped mechanism with constant cross-section, Fig. 9. The mechanism is to consists of three compliant links with lengths L_i, i=1,2,3, where the first is clamped and forms an angle of 90° with the second link. Between the second and the last link the angle is (180° - α). These determinations are freely chosen and are taken into account when finding cutting forces and moments. Each section L_i is assigned δ_i, i=1,2,3 and the first equation from (13) is written down. For the geometric parameters a, b and c, the following simple geometric relationships are used:

$$\begin{aligned} a^2 &= (\delta_1 L_1)^2 + (L_2(1-\delta_2))^2, \\ b^2 &= (\delta_2 L_2)^2 + ((1-\delta_3)L_3)^2 - 2\delta_2(1-\delta_3)L_2 L_3 \cos(\pi-\alpha), \\ c^2 &= ((1-\delta_1)L_1 \cos\alpha - L_2 \sin\alpha)^2 + \\ &\quad + (\delta_1 L_1 \sin\alpha + L_2 \cos\alpha + (1-\delta_3)L_3)^2. \end{aligned} \tag{20}$$

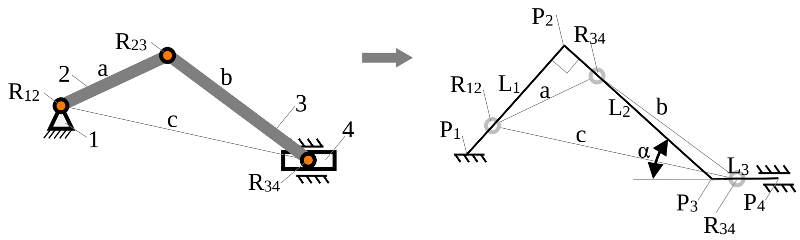

Fig. 9 – Rigid-body mechanism (left) as a model of a compliant beam-shaped mechanism (right).

Using these six algebraic equations and using the desired material parameter *E*, the dimensions of the cross section *h* and *w* and the dimensions *a*,*b*,*c* (21), six parameters L_i and δ_i. i=1,2,3 can be found.

$$\begin{aligned} &w = 5\ \text{mm}, \quad h = 3\ \text{mm}, \quad F = 80\ N, \quad \alpha = 60°, \\ &a = 60\ \text{mm}, \quad b = 100\ \text{mm}, \quad c = 160\ N. \end{aligned} \tag{21}$$

The parameters found are as follows:

$$\begin{aligned} &L_1 \approx 57.5\ \text{mm}, \quad L_2 \approx 127.9\ \text{mm}, \quad L_3 \approx 132.8\ \text{mm}, \\ &\delta_1 \approx 0.05, \quad \delta_2 \approx 0.6, \quad \delta_3 \approx 0.5. \end{aligned} \tag{22}$$

These parameters determine the final geometry of the compliant mechanism. The mechanism deforms under the action of the given force in such a way that the ends of the compliant links rotate around the points R_{12}, R_{23}, R_{34}, Fig. 10. The testing by the linear theory gives an exact agreement of the results.

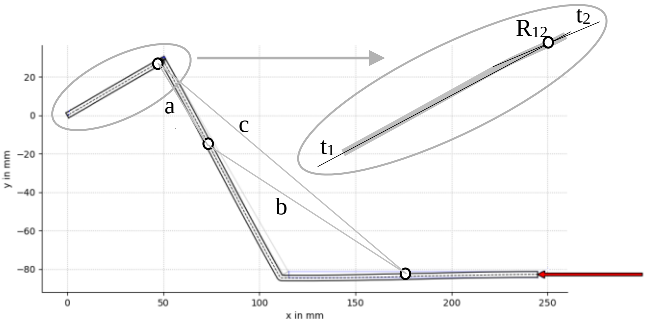

Fig. 10 – Validation of the results through the application of non-linear theory (CoMUI tool).

The application of the non-linear theory (tool CoMUI) provides deviations for the position of the rotation points below 1 mm. The intersection points of the tangents to the section ends L_i were formed, their coordinates were calculated and compared with the coordinates from the linear theory.

From the other additional conditions, such as limitation of the maximum strain, other parameters, for example *h*, *w* or *E* can also be determined using this method.

4. VERIFICATION OF THE NON-LINEAR ANALYTICAL MODEL

In this section, the non-linear analytical model is verified on the example of two different compliant mechanisms with concentrated, Fig. 11 (a), (b), and a mechanism with distributed compliance, Fig. 11 (c).

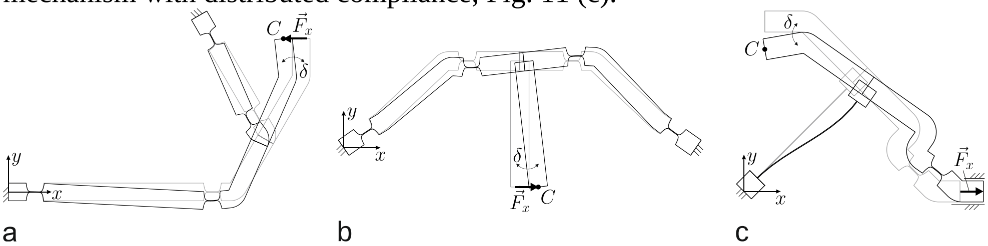

Fig. 11 – Compliant point guidance mechanisms (a) EVANS mechanism and (b) ROBERTS mechanism with 2nd order power function-based contours, (c) slider-crank mechanism with distributed compliance and an 8th order power function-based contour.

The verification is carried out by means of 3D FE analysis using *Solid 186* elements with a mesh refinement at the compliant segments. All three mechanisms represent common kinematics in precision engineering as they can realize a straight-line guidance of a coupler point *C*. Due to the precision, the evaluation of the displacement of point *C* in *x*- (u_{xC}) and *y*-direction (u_{xC}) is suitable for comparing the analytical and FE model. Furthermore, the resulting input force F_{xC} and the rotation angle δ of the coupler are investigated. The EVANS mechanism is deflected by -10 mm, the ROBERTS mechanism by 10 mm and the slider-crank mechanism by a force of F_x=1.5 N. Results for the chosen deflections are given in Table 4 and Table 5.

Table 4

Results for the compliant EVANS and ROBERTS mechanisms.

	F_x in N			u_{yC} in µm			δ in °		
	FEM	Ana.	Δ_{FEM} in %	FEM	Ana.	Δ_{FEM} in %	FEM	Ana.	Δ_{FEM} in %
(a)	-8.59	-8.23	-4.19	-60.65	-60.39	-0.43	6.36	6.36	/
(b)	6.63	6.37	-3.92	-14.95	-15.15	1.34	6.58	6.58	/

Table 5

Results for the compliant slider-crank mechanism.

	u_{xC} in µm			u_{yC} in mm			δ in °		
	FEM	Ana.	Δ_{FEM} in %	FEM	Ana.	Δ_{FEM} in %	FEM	Ana.	Δ_{FEM} in %
(c)	-9.4	-9.9	5.32	-12.89	-13.18	2.25	9.67	9.88	2.17

In summary, both methods coincide well for the chosen mechanisms. Even very small absolute values in the micrometer range can be accurately determined using the analytical model. The maximum deviations of up to 5.5 % result due to the small absolut values and can be reduced to 3 % when the aspect ratios of the flexure hinges are considered and lateral contraction is taken into account as shown in [10].

5. SUMMARY

In this paper, two methods for the synthesis of compliant mechanisms were presented. Both methods are based on replacing the rigid-body mechanisms with the partial or complete compliant mechanisms. In the first method, non-linear theory of curved beams is used. Linear theory is used as the basis for the second method. Table 6 lists the resulting features of the methods and the mechanisms to be obtained, as well as their areas of application with examples.

Table 6

Features of the synthesis methods and mechanisms.

Features	Method 1	Method 2
Kind of mechanisms	Mechanisms with concentrated compliance	Mechanisms with distributed and concentrated compliance
Deformations of mechanisms	Small and large deformations	Primarily small deformations
Solution of model equations	Numerical solutions	Analytical solutions
Function of mechanisms	Mechanisms to realize a desired path or a given displacement	Mechanisms for the realization of the desired relative movements with a given load
Applications / examples	Precision applications, measurement applications, technical systems in which rigid-body mechanisms can be replaced by compliant mechanisms / positioning systems, compliant element on which the forces to be measured act ([11], [12]), compliant elements in technical devices	Medicine technical applications, robotics, gripper technology, technical systems in which rigid-body mechanisms can be replaced by compliant mechanisms / compliant gripper, robot, medical probe, compliant elements in technical devices

The mechanisms as a result of one of the methods shown can be checked for their deformation behavior using the tool CoMUI. Moreover, the tool can be used to initiate optimization steps with respect to selected geometric and/or material parameters in order to improve the results as desired. The validation of the non-linear method, which is the basis of this tool, shows a good correlation with the FE method with displacement deviations lower than 5.5 %.

Acknowledgments: The authors gratefully acknowledge the support of the Carl Zeiss Foundation.

REFERENCES

1. GALLEGO, J.A., HERDER, J., *Synthesis Methods in Compliant Mechanisms: An Overview*, Proceedings of the ASME 2009 International Design Engineering Technical Conferences and Computers and Information in Engineering Conference, **7**, 33rd Mechanisms and Robotics Conference, Parts A and B, San Diego, California, USA, August 30–September 2, 2009, pp. 193–214. ASME, 2009, doi: 10.1115/DETC2009-86845
2. BILANCIA, P., BERSELLI, G., *An Overview of Procedures and Tools for Designing Nonstandard Beam-Based Compliant Mechanisms*, Computer-Aided Design, **134**, 2021, 103001, doi: 10.1016/j.cad.2021.103001
3. TIAN, Y., SHIRINZADEH, B., ZHANG, D., *Closed-form compliance equations of filleted V-shaped flexure hinges for compliant mechanism design*, Precis. Eng., **34**, *3*, pp. 408–418, 2010, doi: 10.1016/j.precisioneng.2009.10.002
4. BERGLUND, M. D., MAGLEBY, S. P., HOWELL, L. L., *Design Rules for Selecting and Designing Compliant Mechanisms for Rigid-Body Replacement Synthesis*, Proceedings of the ASME 2000 International Design Engineering Technical Conferences and Computers and Information in Engineering Conference, **2**, 26th Design Automation Conference. Baltimore, Maryland, USA, September 10–13, ASME, pp. 233–241, 2000, doi: 10.1115/DETC2000/DAC-14225
5. KIM, C., *Decomposition Strategies for the Synthesis of Single Input-Single Output and Dual Input-Single Output Compliant Mechanisms*, Proceedings of the ASME 2007 International Design Engineering Technical Conferences and Computers and Information in Engineering Conference, **8,** 31st Mechanisms and Robotics Conference, Parts A and B. Las Vegas, Nevada, USA. September 4–7, ASME, pp. 137–146, 2007, doi: 10.1115/DETC2007-35449
6. KIRMSE, S., CAMPANILE, L. F., HASSE, A., *Synthesis of compliant mechanisms with selective compliance – An advanced procedure*, Mech. Mach. Theory **157**, 2021, 104184, doi: 10.1016/j.mechmachtheory.2020.104184
7. LIU, K., TOVAR, A., *An efficient 3D topology optimization code written in Matlab*, Struct. Multidiscipl. Optim., **50**, *6*, pp. 1175–1196, 2014, doi: 10.1007/s00158-014-1107-x
8. ZENTNER, L., LINß, S., *Compliant systems: mechanics of elastically deformable mechanisms, actuators and sensors*, Berlin: De Gruyter, 2019, ISBN 3-11-047731-9
9. HENNING, S., LINß, S., ZENTNER, L., *detasFLEX - A computational design tool for the analysis of various notch flexure hinges based on non-linear modelling*, Mechanical sciences, Mech. Sci., **9**, *2*, pp. 389–404, 2018, doi: 10.5194/ms-9-389-2018
10. HENNING, S., ZENTNER, L., *Analysis of planar compliant mechanisms based on non-linear analytical modeling including shear and lateral contraction*, Mech Mach Theory, **164**, 2021, 104397, doi: 10.1016/j.mechmachtheory.2021.104397
11. SCHLEICHERT, J., RAHNEBERG, I., MARANGONI, R. R., FRÖHLICH, T., *Calibration and uncertainty analysis for multicomponent force/torque measurements*, tm - Technisches Messen, **84**, *2*, pp. 130–136, 2017, https://doi.org/ 10.1515/teme-2016-0048
12. MARANGONI, R. R., SCHLEICHERT, J., RAHNEBERG, I., MASTYLO, R., MANSKE, E., FRÖHLICH, T., *Multi-component force measurement in micromachining*, tm - Technisches Messen, **84**, *9*, pp. 587–592, 2017, https://doi.org/10.1515/teme-2016-0066